

# IMPACT OF FADING TIME CORRELATION ON THE PERFORMANCE OF ITERATIVE CHANNEL ESTIMATION FOR CODED OFDM

Giacomo Bacci<sup>\*†</sup>   Antonio Petrolino<sup>◇</sup>   Gonçalo Tavares<sup>◇</sup>   Marco Luise<sup>†</sup>

<sup>\*</sup> Wireless Systems Engineering and Research (WISER) S.r.l., Livorno, Italy

<sup>◇</sup> Inst. Eng. Sist. e Comp. Inv. e Des. (INESC-ID) and Inst. Sup. Técnico (IST), Lisbon, Portugal

<sup>†</sup> Dip. Ingegneria dell'Informazione, University of Pisa, Pisa, Italy

## ABSTRACT

This work studies the impact of a specific channel time correlation model on the link-level performance of a coded OFDM system that uses iterative channel estimation. When the main focus of extensive simulation campaigns is to measure the overall system performance, it would be desirable to implement low-complexity algorithms that replace the well-agreed-upon Clarke's model to mimic the time evolution of the multipath fading process. The main scope of this paper is to investigate suitable scenarios in which this approach is allowed, by using both theoretical analysis and numerical simulations.

## 1. INTRODUCTION

The increasing demand for high-speed mobile wireless communications calls for designing systems with high spectral and energy efficiency. Current solutions to meet this goal are provided by multicarrier OFDM systems, adopted by next-generation wireless standards, such as the IEEE 802.16 [1] and long-term evolution (LTE) [2] ones. Due to the need to support mobile users with broadband services, next-generation systems must be robust to the *double selectivity* of the wireless channel. To improve the system performance while exploiting channel coding, we can combine the soft information from the channel decoder with iterative channel estimation, so as to provide a code-aided turbo architecture [3].

To evaluate its benefits, both frequency and time channel selectivity must be properly modeled according to realistic environments. While multipath profiles are in general provided by the system standards to mimic frequency selectivity, counterparts for the Doppler spectrum, which rules the fading time evolution, are often unspecified. It is common to adopt the Clarke's model<sup>1</sup> [4], in which the statistics of the received signal at the mobile terminal are deduced from uniform scatter modeling. However, due to the complexity in

approximating the non-rational Clarke's spectrum with low-order filters, simulations may turn out to be computationally cumbersome [5]. Hence, a way to mitigate this problem is to simulate simpler Doppler spectra, provided that the overall system performance remains substantially unchanged.

To the best of the authors' knowledge, the impact of the channel autocorrelation function (ACF) on the performance of iterative channel estimation is scarcely investigated in the literature, especially in the case of a code-aided approach.

The goal of this work is to derive an analytical criterion that identifies situations in which the ACF shape has a negligible impact on the system performance, so that an artificial, more computationally convenient ACF can be implemented during simulations without a loss in the performance accuracy. In other words, we investigate Doppler spectra with the goal of selecting those which can be simulated more efficiently than the Clarke's spectrum and provide the same link-level performance. Such desirable cases are derived using theoretical tools, and are confirmed using simulations.

The remainder is structured as follows. Sect. 2 describes the channel model considered for this work. Sect. 3 provides a theoretical analysis of the impact of different ACFs on the system performance, validated in Sect. 4 by means of some simulation results. Finally, Sect. 5 concludes the paper.

## 2. CHANNEL MODEL

The transmission makes use of an OFDM signal, that undergoes a *doubly-selective* channel with additive white Gaussian noise (AWGN). A good model is the wide-sense stationary uncorrelated scattered (WSSUS) model by Bello [6], in which each fading path is modeled as a complex random process uncorrelated with any other path. The channel impulse response  $h(t)$  can be expressed as the tapped-delay line

$$h(t) = \sum_{i=0}^{N_p(t)-1} g_i(t) e^{j\theta_i(t)} \delta(t - \tau_i(t)), \quad (1)$$

where  $\delta(\cdot)$  is the Dirac's delta function, and  $N_p(t)$ ,  $g_i(t)$ ,  $\theta_i(t)$ , and  $\tau_i(t)$  denote the number of paths, attenuation, phase shift, and propagation delay of each path, respectively.

<sup>1</sup>This model is often also referred to as the Jakes' model. Actually, Jakes developed a simulator for generating fading processes according to the model of Clarke.

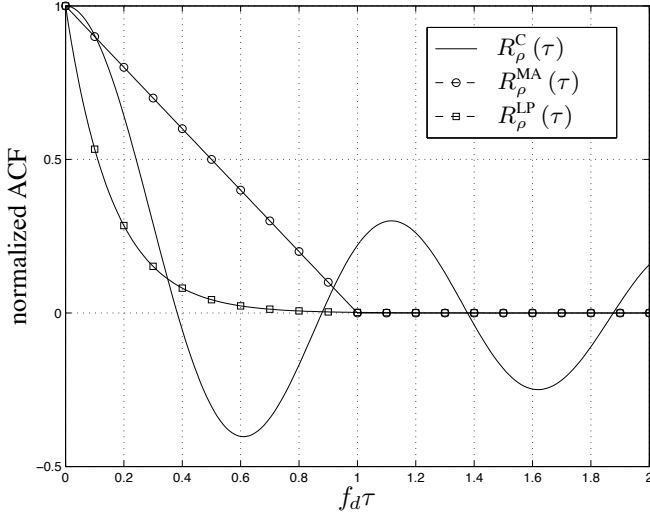


**Fig. 1.** Normalized ACFs versus the normalized delay  $f_d \tau$ .

Since the model by Bello assumes the paths to be uncorrelated, we can focus on the  $i$ -th path  $\rho_i(t) = g_i(t) e^{j\theta_i(t)}$ . When a line-of-sight (LOS) path is not available,  $g_i(t)$  is well modeled by a Rayleigh distribution, whereas  $\theta_i(t)$  is uniformly distributed in  $[0, 2\pi)$ . The time evolution of  $\rho_i(t)$  is ruled by its ACF, which is a function of the maximum Doppler shift  $f_d$  and whose behavior depends on the propagation model. For simplicity, we consider all the paths to show the same normalized ACF, i.e.,

$$R_{\rho_i}(\tau) = \mathbb{E}\{\rho_i(t+\tau)\rho_i^*(t)\} = \sigma_i^2 R_\rho(\tau), \quad (2)$$

where  $\mathbb{E}\{\cdot\}$  denotes expectation, and  $\sigma_i^2$  is the mean power of the  $i$ -th path. Note that  $\{\sigma_i^2\}$  are normalized so as to fulfill  $\sum_{i=0}^{N_p(t)-1} \sigma_i^2 = 1$ . While  $N_p(t)$ ,  $\{\tau_i(t)\}$ , and  $\{\sigma_i^2\}$  are provided by the system standards,  $R_\rho(\tau)$  is often unspecified. As is customarily done, we consider  $R_\rho^C(\tau) = J_0(2\pi f_d \tau)$  provided by the Clarke's model as the reference ACF, where  $J_0(\cdot)$  denotes the zero-order Bessel function of the first kind. The computer simulation of the paths  $\rho_i(t)$  according to the Clarke's model can be carried out by using a low-complexity algorithm, such as that proposed in [7], based on a modified Karhunen-Loève (KL) expansion.

The main idea behind this paper is to consider alternative ACFs, whose use is legitimate, as far as the link-level analysis of OFDM systems is concerned, under the hypothesis that the overall performance does not change. In particular, we aim at finding ACFs that require a generation process much simpler than that needed to obtain  $R_\rho^C(\tau)$ . The advantage of this approach is a complexity reduction at the link-level simulator. For the sake of presentation, we limit here to consider two different ACFs (Figure 1):

- $R_\rho^{\text{LP}}(\tau) = e^{-2\pi f_d |\tau|}$ , corresponding to the impulse response of a first-order low-pass (LP) filter with  $-3$ -dB bandwidth equal to  $f_d$ ;

**Table 1.** Computational complexity comparison

ACF model	Real operations per sample
Clarke's	29
LP	9
MA	7

- $R_\rho^{\text{MA}}(\tau) = (1 - f_d |\tau|)^+$ , with  $(x)^+$  denoting the maximum between 0 and  $x$ , representing the correlation between the outputs of a moving-average (MA) filter with bandwidth  $f_d$ .

Note that the ACFs  $R_\rho^{\text{LP}}(\tau)$  and  $R_\rho^{\text{MA}}(\tau)$  are not derived from physical-based models. They have been chosen for convenience since both represent the outcomes of two very low-complexity subblocks, while providing larger (MA filter) and smaller (LP filter) values for typical working conditions (i.e.,  $f_d |\tau| < 1$ ). To impose the ACFs  $R_\rho^{\text{LP}}(\tau)$  and  $R_\rho^{\text{MA}}(\tau)$  in a computer simulation, we can implement a digital first-order Butterworth LP filter and a moving average filter, respectively.

To measure the impact in terms of complexity required by the generation of time-varying processes  $\rho_i(t)$ , we can compare the algorithms mentioned above by means of the number of real operations required to obtain one complex sample of a sequence with the desired ACF. The results, listed in table 1, show that the artificial ACF models described above can be simulated with a significantly lower computational effort compared to the Clarke's ACF (9 and 7 real operations per complex sample versus 29). Hence, having an *a priori* knowledge of the cases in which the reference ACF model can be replaced by one of the convenient models in terms of link-level performance appears to be desirable to reduce the computational load of extensive simulation campaigns.

To allow us to possibly use lower-complexity shapes, the next section describes an analytical tool to measure the impact of a generic ACF on the OFDM system performance. This analysis is confirmed by means of simulations in Sect. 4 for the three ACFs selected above (Clarke's, MA-based, and LP-based models).

### 3. IMPACT ON THE SYSTEM PERFORMANCE

At the receiver side, channel equalization is mandatory to mitigate the distortions introduced by the channel. By extracting the pilots embedded in the OFDM format, we can obtain an estimate  $\hat{\mathbf{h}}[n]$  of the vector  $\mathbf{h}[n] = \{h_k[n]\}_{k=1}^{N_s}$ , where  $h_k[n]$  is the channel response of the  $k$ -th subcarrier of the  $n$ -th OFDM symbol, and  $N_s$  is the number of subcarriers. The equalizer can thus elaborate the received samples, and its output is sent to a channel decoder after removing virtual and

pilot carriers. To improve the system performance, we can exploit the soft information from the channel decoder to refine  $\hat{\mathbf{h}}[n]$ . This work considers a joint time-domain Wiener filter (WF), due to its simplicity of implementation while ensuring an optimum minimum mean square error (MMSE) solution. The linear estimator that gives an estimate of  $h_k[n]$  is given by [8]

$$\hat{h}_k[n] = \mathbf{a}_k^H \mathbf{y}_k, \quad (3)$$

where  $(\cdot)^H$  denotes conjugate transposition;  $\mathbf{y}_k$  is a vector containing the  $2L+1$  received samples in the frequency domain centered around the  $k$ -th subcarrier of the current plus the  $S$  past OFDM symbols; and

$$\mathbf{a}_k = [\mathbb{E}\{\mathbf{y}_k \mathbf{y}_k^H\}]^{-1} \cdot \mathbb{E}\{h_k^*[n] \mathbf{y}_k\}. \quad (4)$$

collects the  $(2L+1) \cdot (S+1)$  WF coefficients, with  $L$  and  $S$  being the WF memory in the frequency and time domains, respectively.

Using the MMSE criterion, the WF taps are functions of channel selectivity models, AWGN power, and a-posteriori probabilities of the symbols (see [8] for more details). Since the focus here is on the impact of  $R_\rho(\tau)$  on the OFDM system performance, let us investigate how  $R_\rho(\tau)$  regulates  $\mathbf{a}_k$ . For the ease of presentation, let us assume a WF in the time domain only (i.e.,  $L=0$ ) without data modulation. The following results can be extended to any  $L$  and any quadrature amplitude modulation (QAM) data constellation with some computational effort. The major conclusions derived here are valid for the general case as well. Under these assumptions,

$$\mathbf{a} = [a_0, \dots, a_S]^H = [\mathbf{R}_w + \mathbf{R}]^{-1} \cdot \mathbf{r}, \quad (5)$$

with  $\mathbf{R}_w = \sigma_w^2 \mathbf{I}_{S+1}$ , where  $\mathbf{I}_m$  is the  $m \times m$  identity matrix, and  $\sigma_w^2$  is the AWGN power;  $\mathbf{R}$  is a square matrix of order  $S+1$ , whose  $(l, s)$ -th element is  $[\mathbf{R}]_{l,s} = r_{l-s} \triangleq R_\rho((l-s)T_s)$ ; and  $\mathbf{r}$  is the first column of  $\mathbf{R}$ . Note that we can drop the subscript  $k$  in (5) when assuming no data modulation.

To reduce the computational demand of (5), we can resort to the Levinson-Durbin recursion [9], that yields

$$\mathbf{a} = \mathbf{v}_{S+1}, \quad (6)$$

where  $\mathbf{v}_{\ell+1} = [v_{\ell+1,0}, \dots, v_{\ell+1,\ell}]^H$  is the solution computed at the  $(\ell+1)$ -th step of this algorithm. Note that the subscript  $\ell$  denotes both the step of the algorithm and the size of the vector  $\mathbf{v}$ . The elements of  $\mathbf{v}_{\ell+1}$  can be derived using

$$v_{\ell+1,i} = v_{\ell,i} - \eta_\ell \cdot b_{\ell+1,\ell-i}, \quad 0 \leq i \leq \ell, \quad (7)$$

where  $v_{\ell,\ell} \triangleq 0$  for uniformity of notation, and

$$b_{\ell+1,i} = b_{\ell,i} - \kappa_\ell \cdot b_{\ell,\ell-i}, \quad 0 \leq i \leq \ell, \quad (8)$$

where  $b_{\ell,\ell} \triangleq 0$ ,  $\kappa_\ell \triangleq \beta_\ell / \alpha_\ell$ , and

$$\beta_\ell = \sum_{i=0}^{\ell-1} r_{\ell-i} \cdot b_{\ell,i} \quad (9)$$

$$\alpha_\ell = \sum_{i=0}^{\ell-1} r_i \cdot b_{\ell+1,i}. \quad (10)$$

Finally,  $\eta_\ell$  in (7) can be computed as

$$\eta_\ell = \frac{\sum_{i=0}^{\ell-1} r_{\ell-i} \cdot v_{\ell,i} - r_\ell}{\alpha_{\ell+1}}. \quad (11)$$

To solve (5), it is sufficient to set  $\mathbf{v}_1 = [v_{1,0}] = (1 + \sigma_w^2)^{-1}$  and  $b_{1,0} = 1$ , and to stop the algorithm at  $\ell = S+1$ .

To quantify the impact of  $\{r_i\}$  (and thus the ACF) on  $\mathbf{a}$ , we are interested in evaluating the number of significant coefficients of a hypothetically infinite-tap WF. To this aim, let us suppose (5) to be a linear system with order  $\ell \rightarrow +\infty$ . We can again use the algorithm above, until  $\ell = \ell^*$  is such that

$$|\eta_{\ell^*}| < \varepsilon \cdot \mathbf{1}_{\ell^*}^T \mathbf{v}_{\ell^*}, \quad (12)$$

where  $\varepsilon$  is chosen to be sufficiently small, and  $\mathbf{1}_m$  denotes the  $m \times 1$  all-ones vector. The size  $\ell^*$  is a practical measure for the number of significant coefficients of the infinite-tap filter (i.e., coefficients whose magnitude is at least  $\varepsilon$  times greater than the sum of *all* filter taps). It depends *only* on AWGN power  $\sigma_w^2$ , tolerance  $\varepsilon$  and coefficients  $r_i$ , which are in turn functions of both the ACF and  $f_d$ . Interestingly, although  $\ell^*$  depends on  $R_\rho(\tau)$ , its behavior *cannot* be directly estimated by the bare inspection of  $R_\rho(\tau)$  as a function of  $\tau$ , as will be shown in Sect. 4. Note also that  $\ell^*$  does *not* depend on the channel frequency model and on the receiver parameters.

Computing  $\ell^*$  for a given scenario (i.e.,  $R_\rho(t)$  and  $f_d$ ) is expedient to derive the following considerations. If  $S \geq \ell^*$ ,  $|a_s| \approx 0$  for  $\ell^* \leq s \leq S$ . Hence, the performance achieved by a WF with  $S \geq \ell^*$  is the same of a WF with  $S' = \ell^* - 1$ . Using  $S \geq \ell^*$  thus adds unnecessary complexity to the receiver. On the contrary, if  $S < \ell^* - 1$ , there is still room for estimation improvement by increasing  $S$  up to  $\ell^* - 1$ , since weighing more OFDM symbols yields a more effective AWGN smoothing.

This also allows us to compare the system performance using different ACFs, given the same scenario (order  $S$ , speed  $v$ , AWGN power  $\sigma_w^2$ ). Let us select two generic ACFs  $R_\rho^{(1)}(\tau)$  and  $R_\rho^{(2)}(\tau)$ , with sizes  $\ell_1^*$  and  $\ell_2^*$ , respectively. Without loss of generality, let us assume  $\ell_1^* > \ell_2^*$ . For any  $S$ , the first system is expected to outperform the second one, since OFDM symbols are more correlated ( $\ell_1^* > \ell_2^*$ ). However, the performance gap *does* depend on  $S$ . If  $S < \ell_2^*$ , both systems exploit all  $S$  past OFDM symbols, and the performance is roughly the same. When  $\ell_2^* \leq S < \ell_1^*$ , the WF for the second system weighs only the  $\ell_2^* + 1$  last OFDM symbols, and thus the performance gap increases as  $S$  increases, due to the different AWGN smoothing. The maximum gap occurs when  $S = \ell_1^* - 1$ , and does not increase any further (for  $S \geq \ell_1^*$ ).

The same conclusions apply for a generic frequency-domain order  $L > 0$  when using a joint time-domain WF. The impact of a larger  $L$  is to amplify the gap between different correlation models  $R_\rho(\tau)$ . In practice, as we will see in the next section, the numerical performance gaps are also impacted by the forward error correction (FEC) coding and the

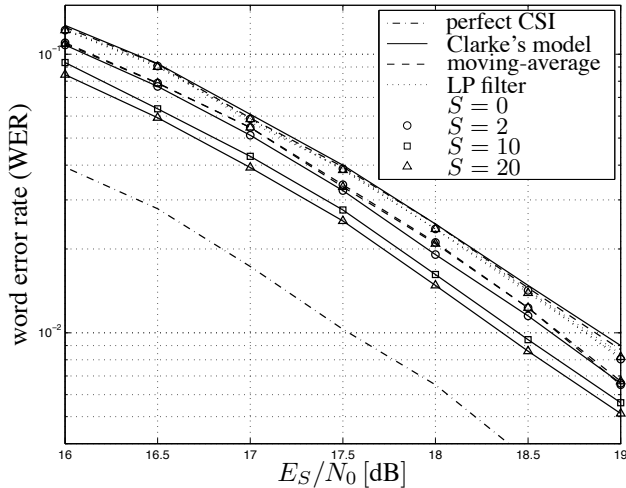


**Fig. 2.** WER performance as a function of  $E_S/N_0$  for different time-domain filter order  $S$  ( $L = 1$ ,  $v = 90$  km/h).

effect of  $M$ -QAM data modulation. However, if a selected scenario provides  $S < \ell_2^* < \ell_1^*$ , we can indifferently use  $R_\rho^{(1)}(\tau)$  and  $R_\rho^{(2)}(\tau)$  from the link-level performance point of view, since both ACFs will provide the same results with an excellent approximation.

Note that the analysis presented in this section can be extended to any other iterative channel estimator and any other ACF. This can be done by identifying the dependence of the estimator coefficients on the samples of the ACF, as we have done above by re-interpreting the vector  $\mathbf{a}$  in (5) as the iterative solution of the Levinson-Durbin algorithm (6).

#### 4. NUMERICAL RESULTS

The frame used to evaluate the link-level performance is based on the IEEE 802.16m time division duplex (TDD) downlink frame [1]. The relevant parameters are:  $N_s = 1024$  subcarriers; sampling frequency  $f_s = 11.2$  MHz; OFDM symbol duration  $T_s = N_s/f_s \simeq 0.1$  ms; and carrier frequency  $f_0 = 3.5$  GHz. We use a nonbinary(NB)-LDPC coding scheme, with codewords of  $N = 360$  coded symbols in the Galois field  $\text{GF}(64)$  [10] and rate  $1/2$ , using the parity check matrices derived in [11]. The I/Q modulation considers a 64-QAM constellation, the channel equalizer adopts a zero-forcing (ZF) strategy, and the 24-tap ITU modified vehicular-A channel profile [12] is used to model the frequency selectivity, which implies  $N_p(t) = 24$  and provides specific values for  $\{\tau_i(t)\}$  and  $\{\sigma_i^2\}$ .

Figure 2 shows the experimental word error rate (WER) as a function of the signal-to-noise ratio (SNR)  $E_S/N_0$ . The transmitter-receiver speed is  $v = 90$  km/h, which yields  $f_d \simeq 291$  Hz, and a coherence time  $T_c \simeq 15T_s$ . Hence, this scenario bears a mild yet nonnegligible time selectivity. Using the analysis of Sect. 3 with  $\varepsilon = 0.01$  in the SNR range  $16 \div 19$  dB,

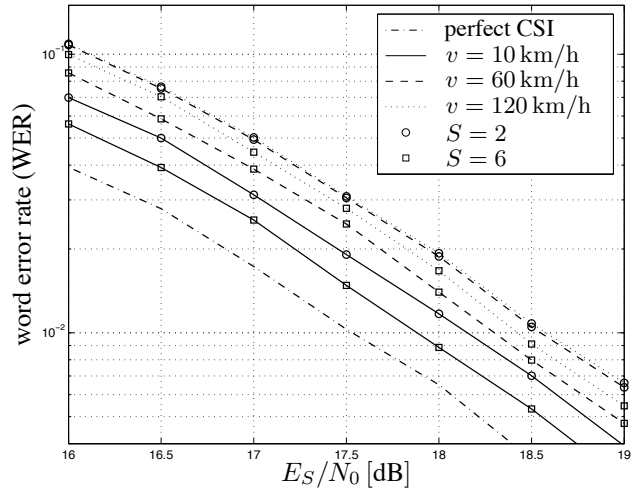


**Fig. 3.** WER performance for different time-domain filter order  $S$  and different speeds (Clarke's model,  $L = 1$ ).

$\ell^* = \{18, 2, 1\}$  for Clarke's, MA- and LP-based models, respectively. We thus expect similar performance only when  $S \leq 2$ . To this aim, we consider  $S = \{0, 2, 10, 20\}$  and  $L = 1$ . Solid, dashed, and dotted lines refer to Clarke's, MA-, and LP-based ACFs, respectively. For the sake of completeness, the dash-dotted line represents the WER performance with perfect channel knowledge. As can be seen, the results for  $S \geq 2$  overlap for  $R_\rho^{\text{MA}}(\tau)$  and  $R_\rho^{\text{LP}}(\tau)$ , whereas they improve as  $S$  increases for  $R_\rho^{\text{C}}(\tau)$ , up to  $S = \ell^* - 1 = 17$ .

An analogous investigation, using  $L = 1$ , is conducted for three different scenarios:  $v = 10$  km/h (weak selectivity);  $v = 60$  km/h (mild selectivity); and  $v = 120$  km/h (severe selectivity). For the ease of presentation, only  $S = \{2, 6\}$  is considered. Figure 3 reports the experimental WER assuming the time selectivity to be ruled by the Clarke's model  $R_\rho^{\text{C}}(\tau)$ , whereas Figure 4 adopts  $R_\rho^{\text{MA}}(\tau)$  as the multipath ACF. Let us focus on  $R_\rho^{\text{C}}(\tau)$  first. By setting  $\varepsilon = 0.01$ , we get  $\ell^* = \{43, 25, 14\}$  for  $v = \{10, 60, 120\}$  km/h, respectively. Hence, we expect the WER to decrease in all the scenarios when increasing  $S$  from 2 to 6. Due to the decreasing behavior of  $\ell^*$  with  $v$ , the benefits from higher  $S$  are expected to be more apparent with lower speeds, as confirmed by the numerical results. When assuming  $R_\rho^{\text{MA}}(\tau)$  as the ACF, the qualitative behavior is confirmed, although the gap between  $S = 2$  and  $S = 6$  becomes slighter, especially for high speeds. When  $\varepsilon = 0.01$ ,  $\ell^* = \{5, 2, 1\}$  for  $v = \{10, 60, 120\}$  km/h, respectively. Hence, the WER performance improves only in the case  $v = 10$  km/h, as can be seen in Figure 4. Note that, when  $v$  increases (and thus the correlation between subsequent OFDM symbols decreases),  $R_\rho^{\text{MA}}(\tau)$  performs similarly to  $R_\rho^{\text{C}}(\tau)$  when low values for  $S$  are used. This is particularly apparent when  $v = 120$  km/h and  $S = 2$ , but holds even for  $v = 60$  km/h,  $S = 2$ . On the contrary, when  $S = 6$  and/or  $v = 10$  km/h, the perfor-

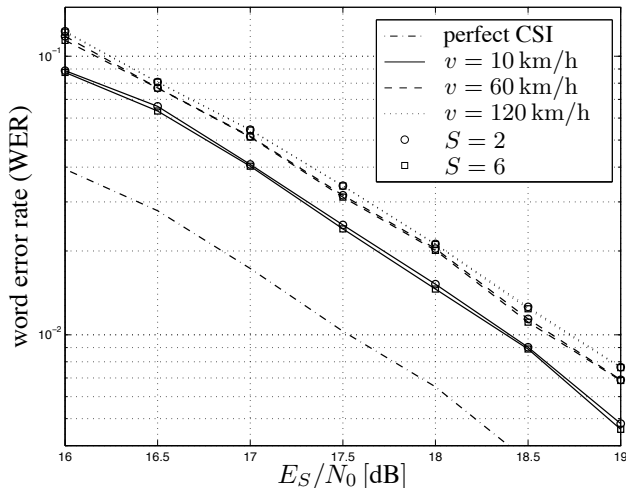


**Fig. 4.** WER performance for different time-domain filter order  $S$  and different speeds (MA model,  $L = 1$ ).

mance loss of the MA-based scenario is significantly worse, although in the latter case (in which  $f_d T_s \simeq 3 \times 10^{-3}$ ) the coefficients  $r_i$  of the MA model are very similar to the Clarke's ones (see Figure 1). The same conclusions apply even more clearly for the LP-filter-based model, in which  $\ell^* = \{2, 1, 1\}$  for  $v = \{10, 60, 120\}$  km/h, respectively (not reported here for the sake of brevity).

## 5. CONCLUSION

This paper investigates the impact of the fading time autocorrelation functions (ACFs) on the end-to-end performance of a coded OFDM transmission scheme in which an iterative Wiener-filter-based channel estimation is used to exploit the soft information from the receiver decoder. The main scope is to investigate the possibility of adopting ACF models that allow the simulation of channel time selectivity with computationally efficient methods - more efficient than those required for the simulation of the Clarke's model. We showed that, in some practical situations, the adoption of the Clarke's ACF results in better performance than other ACFs, including those obtained with low-pass filters with bandwidth equal to the maximum Doppler shift. Hence, alternative, computationally efficient ACFs must be used carefully, since in some cases the system performance proves to be significantly different from that expected if the actual ACF follows the Clarke's model. However, under special conditions, such as low time-domain Wiener filter orders and average-to-high speeds, the end-to-end performance does not change significantly. In this case, using low-complexity models, such as the moving-average and the low-pass-filter-based ones, yields the same link-level performance with a channel generation process up to four time faster than that required for the Clarke's counterpart.

## 6. REFERENCES

- [1] IEEE 802.16 Broadband Wireless Access Working Group, "IEEE 802.16m System Description Document (SDD)," *Tech. Rep. IEEE 802.16m-09/0034r2*, Sept. 2009.
- [2] 3GPP Technical Specification Group, "Radio Access Network; Evolved Universal Terrestrial Radio Access (E-UTRA); LTE Physical Layer - General Description (Release 8)," *Tech. Rep. 3GPP TS36.201 v8.1.0*, Nov. 2007.
- [3] C. Douillard, M. Jézéquel, C. Berrou, A. Picart, P. Didier, and A. Glavieux, "Iterative correction of intersymbol interference: Turbo-equalization," *Eur. Trans. Commun.*, vol. 6, no. 5, pp. 507–511, Sept.–Oct. 1995.
- [4] R. Clarke, "A statistical theory of mobile radio reception," *Bell System Technical J.*, vol. 47, no. 6, pp. 957–1000, July–Aug. 1968.
- [5] C. Kominakis, "A fast and accurate Rayleigh fading simulator," in *Proc. IEEE Global Telecommunications Conference (GLOBECOM)*, San Francisco, CA, Dec. 2003, pp. 3306–3310.
- [6] P. Bello, "Characterization of randomly time-variant linear channels," *IEEE Trans. Commun.*, vol. 11, no. 4, pp. 360–393, Dec. 1963.
- [7] A. Petrolino, J. Gomes, and G. Tavares, "A mobile-to-mobile fading channel simulator based on an orthogonal expansion," in *Proc. IEEE Veh. Technol. Conf.*, Marina Bay, Singapore, May 2008, pp. 366–370.
- [8] G. Bacci, M. D. Maggiora, and M. Luise, "Iterative channel estimation for non-binary LDPC-coded OFDM signals," in *Proc. IEEE Int. Workshop on Signal Processing Advances for Wireless Communications*, Marrakech, Morocco, June 2010.
- [9] S. Haykin, *Adaptive Filter Theory*, 4th ed. Upper Saddle River, NJ: Prentice-Hall, 2002.
- [10] M. Davey and D. MacKay, "Low density parity check codes over  $GF(q)$ ," *IEEE Commun. Lett.*, vol. 2, no. 6, pp. 165–167, June 1998.
- [11] DA VINCI Project Team, "DA VINCI: Design And Versatile Implementation of Non-binary wireless Communications based on Innovative LDPC Codes," *EU-Project INFSCO-ICT-216203*, Nov. 2007.
- [12] IEEE 802.16 Broadband Wireless Access Working Group, "IEEE 802.16m Evaluation Methodology Document," *Tech. Rep. IEEE 802.16m-08/004r5*, Jan. 2009.